

High-resolution atomic force microscope nanotip grown by self-field emission

C. H. Oon and J. T. L. Thong^{a)}

Centre for Integrated Circuit Failure Analysis and Reliability (CICFAR), Faculty of Engineering, National University of Singapore, 4 Engineering Drive 3, Singapore 117576, Singapore

Y. Lei

Singapore-MIT Alliance, 4 Engineering Drive 3, Singapore 117576, Singapore

W. K. Chim

Department of Electrical and Computer Engineering, National University of Singapore, and Singapore-MIT Alliance, 4 Engineering Drive 3, Singapore 117576, Singapore

(Received 11 June 2002; accepted 22 August 2002)

A technique to grow a single tungsten filament tip on a tapping mode atomic force microscope (AFM) tip by a process of self-field emission in the presence of tungsten carbonyl is demonstrated. Such filaments have a tip radius of 1–2 nm and are grown to lengths ranging from 400 nm to 3 μm and a shank diameter of about 60–90 nm. Images of germanium nanocrystals and porous alumina membranes show much higher resolution and definition than standard AFM tips. The tip shows no degradation even after 10 h of scanning, demonstrating its utility as a practical tip. The self-aligned nature of the growth makes it a very simple nanotip fabrication technique. © 2002 American Institute of Physics. [DOI: 10.1063/1.1515120]

The atomic force microscope (AFM) is now considered to be one of the most essential tools in the world of nano-characterization. At the heart of the AFM is the tip that is used to image the sample. Commercial etched silicon tips have tip radii of approximately 10 nm and are generally not suitable for resolving features smaller than 10 nm. Various methods have been developed to produce tips of smaller radius and higher aspect ratio such as electron- and ion-beam induced deposition,^{1–3} focused ion beam milling,⁴ and the use of whiskers.^{5,6} More recent interest in atomic force microscopy involves either attaching or growing a carbon nanotube (CNT) on an etched silicon tip.^{7,8} However the process is difficult and fairly unreliable. Another drawback of using CNTs as AFM tips lies in the inherent property of the CNT—the tip radius is equal to the radius of the CNT shank. To maintain stability, the diameter of the CNT has to be increased along with its length, thereby trading off its lateral resolution. An ideal tip should have a cylindrical shaft of desired length that is sufficiently thick for flexural rigidity, and which tapers off to a cone at the top and ends with a sharp tip. Here, we report a self-aligned technique to grow a tungsten tip on a standard etched silicon AFM tip by a process of field emission in the presence of tungsten hexacarbonyl [$\text{W}(\text{CO})_6$].

It was previously discovered that corona discharge in an ambient of metal carbonyls would result in the growth of needle-like structures at the cathode.^{9,10} However the growth is generally uncontrolled and erratic. By controlling the field-emission current from the cathode,¹¹ which in the present case is a standard AFM tip, it is possible to grow single metallic nanofilaments (Fig. 1). Similar nanofilament growth, attributed to field-induced deposition, has also been

observed on the ends of scanning tunneling microscope (STM) tips used for STM induced deposition.¹² However these filaments, with diameters of typically less than 20 nm, are too thin for use as AFM tips because they do not have sufficient flexural rigidity. However, thicker single filaments can be grown by field emission using a two-step process, described below.

Filament growth is carried out in a Philips XL30 FEG environmental scanning electron microscope (ESEM) that serves no purpose in the growth process itself other than to facilitate alignment of the tip to the anode before growth and subsequent inspection of the tip grown. A metal nozzle connected to an external source of tungsten hexacarbonyl is positioned in the chamber within the field of view of the SEM and serves both as the gas nozzle and the anode. A thin

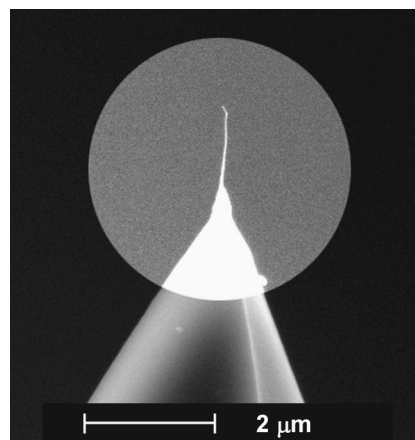


FIG. 1. Tungsten filament grown by field emission from an etched silicon AFM tip. The image contrast in the highlighted circular region is enhanced to show the filament. The original filament diameter is estimated to be less than 15 nm but appears thicker due to contamination buildup during imaging in the SEM.

^{a)}Electronic mail: elett@nus.edu.sg

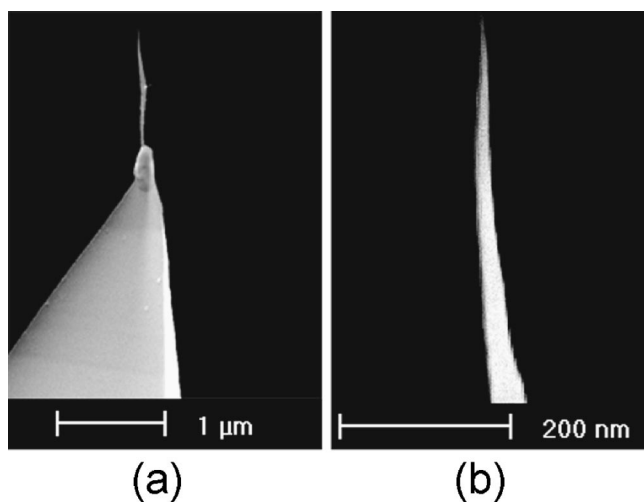


FIG. 2. Thickened filament obtained using two-stage growth. (a) Low-magnification SEM image; (b) higher-magnification image showing details of the tip.

tungsten wire is strung across the opening of the nozzle as a close proximity anode. A silicon tapping-mode AFM tip, sputter coated with gold to improve its conductivity, is positioned approximately $50\ \mu\text{m}$ from the wire. The anode is biased by a high-voltage source that is controlled by a feedback loop such that it operates in constant-current mode upon initiation of filament growth. We have not been successful in using the technique to grow nanotips on standard contact-mode AFM tips because the lower degree of stiffness of such AFM cantilevers results in excessive cantilever deflection when the anode is biased and often the cantilever breaks.

The tip is made to field emit for a few seconds in a tungsten hexacarbonyl ambient at $100\ \text{nA}$ in constant-current mode. The pressure at the nozzle is estimated to be around $1\ \text{mbar}$. A filament is grown when the necessary voltage to sustain field emission is rapidly reduced to about $90\ \text{V}$. At this stage, the filament is typically less than $5\ \text{nm}$ in diameter and a few hundred nanometers in length. The current is then abruptly increased to $4\ \mu\text{A}$ and linearly ramped to $10\ \mu\text{A}$ over a period of $1.5\ \text{s}$ and then ramped down again to $4\ \mu\text{A}$ over the same period before terminating emission. The first procedure is to obtain single-filament growth in order to confine the field emission to a single point. The second procedure thickens the shank to about $60\ \text{nm}$, from its previous diameter of $3\text{--}4\ \text{nm}$, and increases the length by another few hundred nanometers. This two-step growth is necessary since constant-current growth between $200\ \text{nA}$ and $3\ \mu\text{A}$ tends to result in forking and the formation of multiple tip ends. By virtue of the fact that the tip initiates at the point of field emission, the nanotip is self-aligned to the tip of the tapping mode probe as shown in Fig. 2.

Energy dispersive x-ray analysis on similarly grown structures indicates the material to be at least $80\ \text{at.}\%$ tungsten with the balance carbon. The tips do not oxidize in air due to the amorphous carbon overcoat along its entire length.¹¹ The length of the nanotip is approximately $1.1\ \mu\text{m}$ while its shape is approximately that of a cone attached to a slightly tapered $600\ \text{nm}$ long cylinder. The aspect ratio of the conical part is $8:1$ while the overall aspect ratio is $18:1$. Even

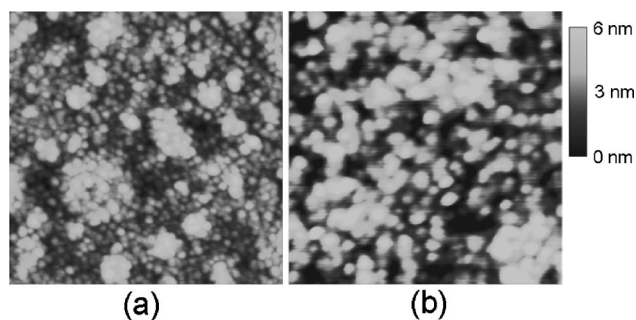


FIG. 3. Tapping-mode AFM image of germanium nanoparticles using (a) a nanotip and (b) a standard etched silicon tip. Horizontal field width = $500\ \text{nm}$.

longer tips have been grown that had an overall length of $3\ \mu\text{m}$ and a base diameter of $90\ \text{nm}$, producing a tip with an aspect ratio of $33:1$.

Two samples are used to compare the performance of this tip versus that of a standard tapping-mode tip (Digital Instruments TESP tip). The first sample comprises germanium nanoparticles of about $6\text{--}10\ \text{nm}$ on silicon dioxide. The second sample is a porous alumina membrane with pore sizes of about $50\ \text{nm}$ and interpore spacing of $115\ \text{nm}$. The scans were carried out at $1\ \text{Hz}$ scan rate, using tapping mode for both tips.

Using the nanotip, scans of the germanium sample show much higher resolution, with individual nanoparticles appearing distinctly in clusters at scan sizes of $500\ \text{nm}^2$ [Fig. 3(a)]. With the standard tip, the clustered nanocrystals are imaged as single entities with no distinction between particles [Fig. 3(b)]. The improved imaging capability of the nanotip is attributed to the very small tip diameter that allows it to penetrate the deep crevices in between particles. Measurements of particle sizes using the standard tip indicate sizes between 15 and $20\ \text{nm}$ as compared to less than $10\ \text{nm}$ using the nanotip. The difference in germanium nanocrystal size is consistent with the estimated tip radii of about $10\ \text{nm}$ for the standard tip and about a few nm for the nanotip. Transmission electron microscope images of similar tungsten filaments grown by the same technique shows tip radii of between 1 and $2\ \text{nm}$.

Since the tip length can easily be varied by changing the growth time, a comparison between two nanotips of differing length ($400\ \text{nm}$ and $3\ \mu\text{m}$) shows that the longer tip is more prone to closed-loop scan instabilities. Such instabilities appear as occasional lateral vibrations while scanning. However the resolution of the long tip does not otherwise appear significantly poorer than that of the short tip. The theoretical first-order resonant frequency of the $3\ \mu\text{m}$ long tip, modeled as a clamped rod and based on the bulk material properties of tungsten, is estimated to be about $5.5\ \text{MHz}$. Since the tapping frequency of the tip is around $300\ \text{kHz}$, any induced flexural vibration of the tip can be quite significant relative to the resolution of the AFM. A shorter tip is desirable if stability is of utmost concern. No significant degradation in tip performance was observed even after $10\ \text{h}$ of use because of the superior mechanical properties of tungsten.

Scans of pore-widened porous alumina membranes sputter coated with gold using the nanotip [Fig. 4(a)] show the cell wall to be much thinner than scans by a standard tip.

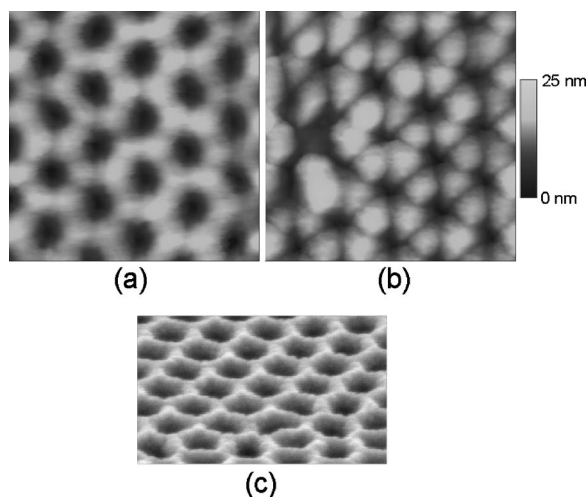


FIG. 4. Tapping-mode AFM image of gold-coated pore-widened porous alumina membrane using (a) a nanotip and (b) a standard etched silicon tip. (c) SEM image of the same sample taken at 60° specimen tilt angle. Horizontal field width = 500 nm.

Scans of the membrane by a normal tip also show significant artifacts, with the cell walls exhibiting round globular structures [Fig. 4(b)]. Inspection by SEM shows that the membrane surface topography is faithfully reproduced by the nanotip, but not by the standard tip [Fig. 4(c)]. It is believed that the globular structures result from convolution of the pyramidal shape of the scanning tip with the periodic surface features. The high aspect ratio structure of the alumina membranes is more clearly shown by the nanotip due to its high aspect ratio and smaller tip radius.

In summary we have developed a self-aligned technique to grow a high aspect ratio high-resolution tip on a standard tapping-mode tip. The procedure is simple and can easily be performed in a simple vacuum system if *in situ* SEM inspection is not required. Metals other than tungsten can be deposited from the appropriate carbonyl for other scanning probe microscopy applications, such as cobalt for magnetic force microscopy.

- ¹K. L. Lee, D. V. Abraham, F. Secord, and L. Landstein, *J. Vac. Sci. Technol. B* **9**, 3562 (1991).
- ²J. E. Griffith, D. A. Grigg, M. J. Vasile, P. E. Russell, and E. A. Fitzgerald, *J. Vac. Sci. Technol. B* **9**, 3586 (1991).
- ³U. A. Griesinger, C. Kaden, N. Lichtenstein, J. Hommel, G. Lehr, R. Bergmann, A. Menschig, H. Schweizer, H. Hillmer, H. W. P. Koops, J. Kretz, and M. Rudolph, *J. Vac. Sci. Technol. B* **11**, 2441 (1993).
- ⁴M. J. Vasile, D. Grigg, J. E. Griffith, E. Fitzgerald, and P. E. Russell, *J. Vac. Sci. Technol. B* **9**, 3569 (1991).
- ⁵E. I. Givargizov, A. N. Stepanova, L. N. Obolenskaya, E. S. Mashkova, V. A. Molchanov, M. E. Givargizov, and I. W. Rangelow, *Ultramicroscopy* **82**, 57 (2000).
- ⁶A. Rothschild, S. R. Cohen, and R. Tenne, *Appl. Phys. Lett.* **75**, 4025 (1999).
- ⁷H. Dai, J. H. Hafner, A. G. Rinzler, D. T. Colbert, and R. E. Smalley, *Nature (London)* **384**, 147 (1996).
- ⁸C. V. Nguyen, K. J. Chao, R. M. D. Stevens, L. Delzeit, A. Cassell, J. Han, and M. Meyyappan, *Nanotechnology* **12**, 363 (2001).
- ⁹H. B. Linden, E. Hilt, and H. D. Beckey, *J. Phys. E* **11**, 1033 (1978).
- ¹⁰F. Okuyama, *J. Appl. Phys.* **53**, 6226 (1982).
- ¹¹J. T. L. Thong, C. H. Oon, M. Yeadon, and W. D. Zhang (unpublished).
- ¹²A. D. Kent, T. M. Shaw, S. von Molnar, and D. D. Awschalom, *Science* **262**, 1249 (1993).